

# 1 Cell free expression in proteinosomes prepared from native protein-PNIPAAm

## 2 conjugates

3 Mengfei Gao, Dishi Wang, Weihua Leng, Michaela Wilsch-Bräuninger, Jonathan  
4 Schulte, Nina Morgner, Dietmar Appelhans and T-Y. Dora Tang\*

## 6 Abstract:

8 Towards the goal of building synthetic cells from the bottom-up, the  
9 establishment of micrometer-sized compartments that contain and support cell free  
10 transcription and translation that couple cellular structure to function is of critical  
11 importance. Proteinosomes, formed from crosslinked cationized protein-polymer  
12 conjugates offer a promising solution to membrane-bound compartmentalisation with  
13 an open, semi-permeable membrane. Critically, to date, there have been no  
14 demonstration of cell free transcription and translation within water-in-water  
15 proteinosomes. Herein, we present a novel approach to the fabrication of  
16 proteinosomes directly from native protein-polymer (BSA-PNIPAAm) conjugates. We  
17 show that these native proteinosomes offer an excellent alternative as artificial cell  
18 chassis. Significantly, the native proteinosomes are stable under high salt conditions  
19 and can consequently support cell free transcription and translation. The native  
20 proteinosomes offer enhanced protein expression compared to proteinosomes  
21 prepared from traditional methodologies. Furthermore, we demonstrate the integration  
22 of proteinosomes into higher order cellular architectures with membrane free  
23 compartments and liposomes. The integration of bioinspired architectural elements  
24 with the central dogma is an essential building block for realizing minimal synthetic  
25 cells and is key for exploiting artificial cells in real-world applications.

27 **Keywords:** (up to 6) proteinosome, cell free expression, artificial cell

## 30 Introduction:

31 A grand challenge in synthetic biology is the bottom-up construction of synthetic  
32 cells that have life-like properties. The integration of bioinspired architectural elements  
33 with enzymatic function is a minimal requirement for the generation of synthetic cells.

34 Thus, the facile establishment of micrometer-sized compartments which contain and  
35 support cell free expression systems provide the foundation to build robust synthetic  
36 cells with increased functional and structural complexity. A prime example has been  
37 the incorporation of cell free expression systems into lipid vesicles <sup>[1,2]</sup> that have been  
38 pivotal in realizing cellular structure and function in a minimal fashion and has been  
39 an essential foundational technology in synthetic cellular research. This system  
40 provides a lipid bilayer boundary that contains cell free expression system that models  
41 the biological cell with its cell membrane and internalized transcription and translation.  
42 This platform has not only been used to model noise <sup>[3]</sup> and crowding in the biological  
43 cell <sup>[4]</sup> but has also been used as prototype to incorporate higher order cellular  
44 functions such as lipid synthesis<sup>[5,6]</sup> DNA replication<sup>[7]</sup> and protein induced membrane  
45 deformations.<sup>[8]</sup>

46 Notwithstanding lipid vesicles, there have been a variety of different  
47 compartments which can support cell free expression from water-in-water membrane  
48 bound compartments such as polymersomes <sup>[12,13]</sup> to water-in-oil systems such as  
49 surfactant stabilized droplets and Droplet Interface Bilayers (DIBS),<sup>[14]</sup> inorganic  
50 colloidosomes,<sup>[15]</sup> and membrane free systems such as coacervates <sup>[16]</sup> and hydrogel-  
51 based systems <sup>[23]</sup>. These synthetic cellular platforms have been important for  
52 increasing compartment stability *via* polymer stabilization <sup>[17]</sup> for enhancing properties  
53 such as intercellular communication and for integrating higher order cellular  
54 architectures <sup>[18–20]</sup> that can be critical for integrating specific cellular properties into  
55 non-living matter.

56 Despite the growing number of ways to include cell free expression systems  
57 into water-in water membrane bound compartments there remain some challenges  
58 with their utilization as synthetic cellular platforms. Namely, that aqueous membrane-  
59 bound compartments, liposomes and polymerosomes are closed systems which  
60 contain a finite amount of resources. This limits the length of time that expression can  
61 take place and the long-term function of the compartment. The addition of membrane  
62 pores <sup>[9,10]</sup> or light activated lipids<sup>[11]</sup> can tune membrane permeability to external  
63 substrates thus providing more resources to internalized cell free expression systems.  
64 The establishment of these systems are non-trivial and every additional component  
65 increases the molecular complexity of the system and increases the challenges in their  
66 fabrication. Therefore, there is still a necessity for alternative solutions for membrane  
67 bound compartmentalized cell free expression systems that provide new functions and

68 features to increase the flexibility and functionality of synthetic cells. Expanding the  
69 repertoire of synthetic cellular platforms provides the ability to open and extend the  
70 range of applications and functionalities by selecting specific properties as an end user.

71 To this end, proteinosomes are alternative membrane- bound compartments  
72 prepared from protein-polymer conjugates<sup>[19,20]</sup> with membranes that are elastic with  
73 tunable permeability to enzymes or DNA molecules.<sup>[21–24]</sup> Water-in-water  
74 proteinosomes have been shown to support reaction cascades,<sup>[25]</sup> DNA strand  
75 displacement reactions and PEN DNA reactions.<sup>[20,21]</sup> They can be manipulated to  
76 generate multi-compartments systems<sup>[24,26–28]</sup>; and are compatible with natural cells,<sup>[29]</sup>  
77 responsive to stimuli,<sup>[30]</sup> can be chemically tuned to incorporate light activatable sorting  
78 communities<sup>[31]</sup> and produced in a high throughput manner.<sup>[32]</sup> Whilst cell free  
79 expression has been demonstrated within non-crosslinked BSA-PNIPAAm conjugates  
80 in oil<sup>[25]</sup>, there is no example of the cell free expression system within water-in-water  
81 proteinosomes. Integration of cell free expression within water-in-water proteinosomes  
82 provides a viable alternative for a synthetic cellular platform, an open compartment  
83 with a permeable membrane to allow the continuous supply of nutrients to the reaction  
84 site.

85 As described previously, the novelty of production of the proteinosomes lies in  
86 the generation of amphiphilic nanoparticles produced by conjugated protein with poly-  
87 (N-isopropylacrylamide) PNIPAAm. These protein-polymer conjugates provide the  
88 scaffold for the proteinosome by stabilizing water-oil emulsions which are then  
89 covalently crosslinked within the emulsions. Typically, protein- (PNIPAAm) conjugates  
90 are synthesized by cationization of a protein such as bovine serum album (BSA) via  
91 carbodiimide chemistry to increase the number of amine groups on the protein. The  
92 amine groups are used to conjugate end capped mercaptothiazoline- activate  
93 PNIPAAm to the protein and to provide crosslinking sites between the amphipathic  
94 protein-PNIPAAm conjugate to stabilize water-in-oil emulsions. To this end, pegylated  
95 bis(sulfosuccinimidyl)suberate (BS(PEG)<sub>n</sub>) crosslinks the protein-PNIPAAm conjugate  
96 via covalent links between the primary amine on the protein and the BS group. This  
97 provides the structural stability to the membrane. Furthermore, (BS(PEG)<sub>n</sub>) is  
98 commercially available with different PEG lengths which tunes the pore size and  
99 permeability of the membrane<sup>[23]</sup>. Removal of the oil phase and transfer to water  
100 leaves water-in-water crosslinked protein-PNIPAAm compartments.<sup>[32]</sup>

101 Our primary goal was to achieve cell free transcription and translation within  
102 proteinosomes, however, when we produced proteinosomes using the conventional  
103 methods using cationized protein-polymer conjugates we found that the  
104 proteinosomes were not stable in the cell free expression systems, most likely due to  
105 the high salt content of the buffer. The stability could be limited by the protein  
106 cationization step in the preparation of the proteinosome where 1-(3-  
107 Dimethylaminopropyl)-3-ethylcarbodiimide hydrochloride (EDC) reactions are used to  
108 chemically modify the protein to add primary amine groups to aspartic and glutamic  
109 acid groups of the protein. Unfortunately, this process has been shown to denature  
110 enzymes which could affect the stability of the proteinosome.

111 Therefore, to integrate cell free expression systems with proteinosomes, we  
112 removed the cationization step to provide a simplified methodology for proteinosome  
113 preparation. We show that this simplified procedure provides robust proteinosomes.  
114 We exploited the porous membrane of the proteinosome to isolate plasmid DNA and  
115 allow transcription and translation machinery to diffuse across the membrane and  
116 drive transcription and translation within the interior of the proteinosome (See  
117 supplementary methods). We show that DNA and mRNA are retained within the  
118 proteinosome whilst expressed proteins diffuse out of the interior of the proteinosomes.  
119 The ability to encapsulate cell free transcription and translation within proteinosome  
120 will give added value to a synthetic cell community by offering an alternative synthetic  
121 cell chassis with facile methods of formation and an open membrane which can allow  
122 the diffusion of resources to its core. This provides a new platform for establishing  
123 higher order architectural structures, reactions and gene circuits with potential  
124 applications in living technologies.

125

## 126 **Results and Discussions:**

127 Given that cationized proteinosomes were not stable in the high salt buffer used  
128 for cell free expression. We developed a new methodology for the preparation of  
129 proteinosomes to remove the protein cationization step and reduce the excess positive  
130 charges that could hinder cell free transcription and translation (**Figure 1A**). To do  
131 this, we directly conjugated PNIPAAm capped with a mercaptothiazoline terminal  
132 group (**Figure S1, S2**) to the -NH<sub>2</sub> group in lysines on the protein BSA that had not  
133 been subjected to cationization. The native BSA conjugate (nat-BSA-PNIPAAm), was  
134 characterized using Laser Induced Liquid Beam Ion Desorption (LILBID) mass

135 spectrometry (**Figure 1B**) and Dynamic Light Scattering (DLS) to confirm that the  
136 polymer had been conjugated to protein. DLS data showed a difference in size  
137 distribution of the protein conjugate at 20 °C compared to 37 °C for the nat-BSA-  
138 PNIPAAm that was not observed in BSA alone (**Figure S3**). This correlated to the  
139 aggregation of conjugated protein-PNIPAAm conjugates above the melting  
140 temperature of the PNIPAAm chain as previously shown.<sup>[33]</sup> In addition, mass  
141 spectrometry data showed peaks corresponding to BSA (67 kDa) and with peaks at  
142 75, 83, 92 and 101 kDa which correlate to the molecular weight of nat-BSA-  
143 (PNIPAAm)<sub>1</sub>, nat-BSA-(PNIPAAm)<sub>2</sub>, nat-BSA-(PNIPAAm)<sub>3</sub>, nat-BSA-(PNIPAAm)<sub>4</sub>  
144 respectively (**Figure 1B**). Together this data confirmed that PNIPAAm was conjugated  
145 to the protein and the average molecular weight of the PNIPAAm chain was 8.4 kDa.  
146 Given the molecular weight of PNIPAAm by mass spectrometry, we determined the  
147 average molar ratio of BSA: PNIPAAm was 1:5.7 by separately measuring the  
148 concentration of protein by a protein bicinchoninic acid assay and UV spectroscopy  
149 and PNIPAAm by UV absorbance at 300 nm (see materials and methods, **Figure S4**  
150 **Table S1**).

151 Having shown that end-capped mercaptothiazoline-activated PNIPAAm can  
152 directly conjugate to native BSA at a molar ratio of 1:5.7 (BSA:PNIPAAm), we tested  
153 the capability of nat-BSA-PNIPAAm conjugates to be coupled with PEG<sub>2000</sub> *via* a bis(N-  
154 succinimidyl succinate) group (BS(PEG)<sub>2000</sub>) to generate crosslinked membrane  
155 bound compartments. Nat-BSA-PNIPAAm was diluted in sodium bicarbonate solution  
156 and mixed with 2-ethyl-1-hexanol with BS(PEG)<sub>2000</sub> at a volume ratio ( $\phi$ ) of 0.06.  
157 Water-in-oil emulsions were generated by pipetting the mixture 10 times at constant  
158 speed, the dispersion was then left overnight at 8 °C for crosslinking (see materials  
159 and methods). The crosslinked proteinosomes were transferred to water by  
160 centrifuging the dispersion at 3000 rcf and replacing the aqueous volume with 70%  
161 ethanol water, followed by repeated centrifugation and replacement of the aqueous  
162 volume with 50% and then 25% ethanol and water.

163 Optical microscopy images showed spherical proteinosomes indicating that the  
164 native protein polymer conjugates could be crosslinked and were stable in water  
165 (**Figure 1C**). Electron microscopy images obtained from negative staining of the  
166 proteinosomes confirmed that the proteinosomes were globular spheres delineated by  
167 a membrane (**Figure 1D**). Further characterization of proteinosomes embedded in  
168 resin, microtomed and imaged by electron microscopy showed a membrane of

169 approximately 10-20 nm encapsulating a lumen (**Figure 1E**). Given the resolution of  
170 the imaging, the membrane thickness is in the range of single or double protein layers  
171 where the hydrodynamic diameter of BSA is approximately 4 nm. The slightly higher  
172 dimension could be caused by osmium tetroxide “staining” – which will react with the  
173 double-bonds within the proteins and slightly increase the thickness of the membrane  
174 layer. Transmission electron microscopy images also showed presence of small  
175 regions of increased electron density with a diameter of hundreds of nanometers.  
176 These small structures could be attributed to small crosslinked inverted micelles of  
177 protein-PNIPAAm conjugates that form during the preparation stage.

178 Given that stable proteinosomes could be formed from nat-BSA-PNIPAAm, we  
179 next tested the capability of these proteinosomes to support cell free transcription and  
180 translation. To do this, we chose to utilize the porosity of the proteinosome membrane  
181 to contain plasmid DNA and allow the diffusion of the transcription and translation  
182 machinery through the membrane. Therefore, we directly encapsulated circular  
183 plasmid DNA (2.3 MDa) into the proteinosomes by including the plasmid DNA into the  
184 aqueous solution prior to mixing with oil and preparation of emulsions by pipetting (see  
185 materials and methods). After transfer of the proteinosomes into water, EvaGreen dye  
186 (final concentration 10  $\mu$ M) was added to the proteinosomes to image the DNA. Optical  
187 microscopy images showed DNA distributed within the interior of the proteinosomes  
188 (**Figure 1F**). Electron microscopy images of nat-BSA proteinosomes encapsulating  
189 DNA showed small regions of increased electron density attributed to plasmid DNA  
190 which were not present in the empty proteinosomes (**Figure 1H, green arrow**).  
191 Together, these results confirm that DNA could be encapsulated within the nat-BSA  
192 proteinosomes. Comparisons of optical microscopy images with proteinosomes  
193 encapsulating DNA prepared from cationized BSA (BSA-NH<sub>2</sub>) proteinosomes (**Figure**  
194 **1G, Figure S5**) showed regions of high fluorescence intensity which could be  
195 attributed to aggregate formation; a lower encapsulation efficiency and a larger  
196 average size of proteinosome compared to the nat-BSA proteinosomes (**Figure 1F,**  
197 **Figure S6**). It could be possible that DNA interacts with the BSA-NH<sub>2</sub>-PNIPAAm  
198 conjugate which could affect conjugate-conjugate interactions and thus the physical  
199 properties of the proteinosomes.

200 Having confirmed that plasmid DNA could be encapsulated within the native  
201 proteinosomes, we then tested the ability for the native proteinosome to support cell  
202 free transcription and translation. To do this, we added nat-BSA proteinosomes that

203 contained plasmid DNA to PURExpress and monitored transcription of mRNA and  
204 translation of protein in 4  $\mu$ L of sample using a microplate reader (**Figure 2A**). DFHBI  
205 dye was added to the PURExpress to monitor mRNA production *via* a Broccoli RNA  
206 aptamer and protein production was detected *via* the expression of the red fluorescent  
207 protein, mCherry. Our results showed fluorescence increase from mRNA and protein  
208 production (**Figure 2B**). Furthermore, optical microscopy images showed that mRNA  
209 was localized within the proteinosome with increasing fluorescence intensity from  
210 mCherry from 10 to 170 min which is evenly distributed throughout the dispersion  
211 (**Figure 2C**). In order to confirm mCherry expression at low concentrations of  
212 proteinosomes, RFP trap beads were added to the solution on the exterior of the  
213 proteinosomes to capture mCherry protein (**Figure 2D, Movie S1**). Fluorescence  
214 microscopy imaging showed increased DFHBI signal inside the proteinosome (**Figure**  
215 **2E**) and mCherry fluorescence intensity on the RFP trap over time (**Figure 2F**). These  
216 results show that native proteinosomes that encapsulate plasmid can support  
217 transcription and translation.

218 To confirm that protein expression was taking place within the proteinosome,  
219 we undertook two control experiments. First, we gently centrifuged the proteinosomes  
220 to the bottom of an Eppendorf tube and took out the supernatant. The supernatant  
221 was added to PURExpress (1x concentration) and transcription and translation was  
222 monitored using a microplate reader (**Figure S7**). The results showed no fluorescence  
223 intensity from production of mRNA or protein which is commensurate with no  
224 transcription and translation taking place within the supernatant and confirming that all  
225 the DNA was contained within the interior of the proteinosomes. Secondly, plasmid  
226 DNA (2.7 nM) and PURExpress (1x) was gently mixed with empty nat-BSA  
227 proteinosomes and incubated for 3 hours at 37 °C. Confocal imaging of the dispersions  
228 incubated with either EvaGreen dye or DFHBI showed green fluorescence on the  
229 exterior of the proteinosomes with no fluorescence in the interior of the proteinosomes.  
230 This indicates that DNA and mRNA cannot diffuse through the membrane (**Figure S8**)  
231 and in the case where the DNA has been pre-encapsulated within the proteinosomes  
232 the results confirm that both transcription and translation take place within the  
233 proteinosome. Taking into account our earlier results, this shows that DNA and mRNA  
234 are retained within the proteinosome and the protein can diffuse through the  
235 membrane. This feature could be exploited in building communication channels *via*  
236 protein diffusion between proteinosomes.

237 When comparing the ability for BSA-NH<sub>2</sub> proteinosomes to support transcription  
238 and translation to the nat-BSA proteinosomes, we found that BSA-NH<sub>2</sub> proteinosomes  
239 disassembled in 1x PURExpress (**Figure S9**). It is possible that the collapse of the  
240 proteinosome was driven by the high salt content either by driving polymer collapse or  
241 due to specific interactions between the components within PURExpress and the  
242 proteinosomes. An alternative explanation could be attributed to the different elasticity  
243 of the membrane in native and cationized proteinosome that could arise from different  
244 degrees of crosslinking. As the cationized proteinosome have additional NH<sub>2</sub> groups  
245 compared to native protein-polymer conjugates, there are more sites for crosslinking  
246 that could lead to membranes which are less porous and more rigid. The addition of  
247 PURE (1x) to the dispersion of proteinosomes can lead to changes in the membrane  
248 as it responds to a change in the osmolarity. These changes could be more easily  
249 accommodated for by the more porous and flexible membrane of the native  
250 proteinosome. In comparison, the change in the osmolarity led to the collapse and  
251 possible disassembly of the cationized proteinosome. Upon dilution of PURExpress to  
252 0.33x, it was possible to observe intact BSA-NH<sub>2</sub> proteinosomes which supported  
253 mRNA production by fluorescence microscopy. Analysis of these microscopy images  
254 showed that mRNA production was lower in the cationized proteinosome compared to  
255 the native proteinosomes (**Figure 2G, 2H, 2I**). Indeed, fluorescence spectroscopy  
256 experiments showed that expression within the BSA-NH<sub>2</sub> proteinosome was reduced  
257 compared to the nat-BSA proteinosomes (**Figure 2, Figure S10**).

258 To determine, if the reduction of protein expression within the cationized  
259 proteinosome was due to the protein-PNIPAAm conjugate, we incubated 1mg.mL<sup>-1</sup> of  
260 protein-PNIPAAm conjugate (nat-BSA-PNIPAAm or BSA-NH<sub>2</sub>-PNIPAAm) in non-  
261 diluted PURExpress with plasmid DNA coding for mRNA-Broccoli and mCherry.  
262 Microplate experiments showed no significant difference in the production of mRNA  
263 and protein in the presence of BSA-NH<sub>2</sub>-PNIPAAm compared to the nat-BSA-  
264 PNIPAAm (**Figure 3A**). Furthermore, comparisons to the control experiments without  
265 protein-PNIPAAm conjugate showed expression levels in the same order of magnitude.  
266 This suggests that protein expression was affected by the compartmentalization rather  
267 than by the individual protein-PNIPAAm conjugates. Given that both native and  
268 cationized proteinosomes used the same crosslinker the reduction in protein  
269 expression could be due to the ability for the expression machinery to diffuse across

270 the membrane. To test this, we characterized the ability of FITC-labeled dextran (40  
271 to 500 kDa) to permeate through the membranes of native and cationized  
272 proteinosomes (**Figure S11**). For native proteinosomes the molecule weight cut off  
273 for the proteinosomes prepared with BS(PEG)<sub>2000</sub> was between 40 and 70 kDa for  
274 FITC-labeled dextran; for proteinosomes prepared with BS(PEG)<sub>9</sub> the molecular  
275 weight cut off was less than 40 kDa. In comparison, the cationized proteinosomes  
276 showed low retention of 40 kDa FITC-labeled dextran. Our results show that the length  
277 of BS(PEG)<sub>n</sub> affects the partitioning of molecules into the proteinosome as shown  
278 previously [23] and that protein cationization changes the permeability compared to the  
279 native protein. In this case cationized proteinosomes have a lower molecular weight  
280 cut off compared to the native proteinosomes. Even though the T7 polymerase is 99  
281 kDa, our results showed mRNA production in both cationized and native  
282 proteinosomes which suggests that the polymerase can diffuse to the interior of the  
283 proteinosome (**Figure 2H**).

284 Furthermore, we tested the partitioning of fluorescently labeled ribosomes  
285 (**Figure S12**) into cationized and native proteinosomes (see materials and methods).  
286 Confocal microscopy images showed fluorescence from ribosomes within nat-BSA  
287 proteinosomes. In comparison ribosomes were aggregated within the interior of the  
288 BSA-NH<sub>2</sub> proteinosomes or interacting at the surface (**Figure 3B**). This suggests that  
289 the ability for the ribosome to diffuse into the proteinosome where the DNA is located  
290 is affected by the cationization of the protein-PNIPAAm conjugate. This could be due  
291 to a decrease in pore size or surface interactions between the ribosomes and the  
292 proteinosomes. Our results suggest that by tuning the pore size of the proteinosome,  
293 protein expression levels can be regulated.

294 As it had previously been shown that changing the molecular weight of the  
295 BS(PEG)<sub>n</sub> crosslinker could change the molecular weight cut off, [23] we prepared  
296 native proteinosomes with a BS(PEG)<sub>9</sub> crosslinker that encapsulated plasmid DNA  
297 (**Figure S13**). These nat-BSA-BS(PEG)<sub>9</sub> proteinosomes were incubated with 0.5x  
298 PURExpress and transcription and translation were monitored on the microplate  
299 reader for mRNA and protein. Comparison between nat-BSA proteinosomes prepared  
300 with BS(PEG)<sub>9</sub> and BS(PEG)<sub>2000</sub> showed that the mRNA production was comparable  
301 but mCherry production was significantly reduced in the proteinosomes prepared with  
302 the smaller BS(PEG)<sub>9</sub> (**Figure 3C**) when the PURExpress had been diluted by a half.  
303 Confocal microscopy images show that after 1 hr of incubation of the proteinosome

304 with fluorescently labeled ribosomes showed a proportion of proteinosomes had  
305 excluded the ribosomes (**Figure 3B**). Together, our results showed that the exclusion  
306 or inclusion of the ribosome in the proteinosome regulates the amount of protein that  
307 is produced and the exclusion of ribosomes can be attenuated by crosslinker length  
308 and pore size of the proteinosomes or by molecular interactions with cationized  
309 protein-PNIPAAm conjugate.

310 It is interesting to note that nat-BSA proteinosomes prepared with DNA were  
311 stable in water for at least a year (**Figure S14**), at a range of pHs (**Figure S15**) and  
312 more stable than cationized proteinosomes at high osmolarity (**Figure S16**) which  
313 suggests that their applications can be widened beyond cell free transcription and  
314 translation as demonstrated here.

315 Therefore, to validate the versatility of the new method, we tested whether we  
316 could generate stable proteinosomes from GOx without any cationization. To this end,  
317 we conjugated PNIPAAm directly to commercially available GOx and crosslinked them  
318 with BS(PEG)<sub>9</sub> as described for BSA. Imaging using optical microscopy and electron  
319 microscopy (**Figure S17**) showed stable proteinosomes. Further to this, we tested the  
320 reactivity of the nat-GOx proteinosomes by adding a dispersion of the proteinosomes  
321 to a phosphate solution containing Amplex Red and horseradish peroxidase (see  
322 material and methods). D-glucose was added to the reaction mixture at 0-50  $\mu$ M  
323 concentrations and was immediately imaged on a microplate reader. Our results  
324 showed that nat-GOx proteinosomes remained active and provides a validation that  
325 this methodology can be readily transferred to other enzymes whilst maintaining  
326 enzymatic activity (**Figure S17**).

327

### 328 **Conclusions:**

329 In brief, we have adapted the methodology for the production of proteinosomes to  
330 integrate for the first time, cell free transcription and translation into crosslinked  
331 aqueous proteinosomes. We present a new method for the preparation of the  
332 proteinosome that directly conjugates the PNIPAAm to native BSA and glucose  
333 oxidase removing the chemically aggressive protein cationization step. Not only does  
334 this facile method provide a robust protocol which can be readily transferred between  
335 laboratories, it also reduces the number of positive charges on the protein polymer  
336 conjugate. We show that the reduction of the positive charges leads to native  
337 proteinosomes that are more stable to high salt environments compared to the

338 cationized proteinosomes. This is significant because it means that cell free  
339 transcription and translation which requires high salt can be supported in these  
340 stabilized proteinosomes. Indeed, we show that transcription and translation is more  
341 efficient in native proteinosomes compared to cationized proteinosomes. Furthermore,  
342 decreased positive charge increases the diffusion of ribosome into the center of the  
343 proteinosome which is required for the translation process. In the case of the native  
344 proteinosome, the diffusion of ribosome into the interior of the compartment can be  
345 tuned by altering the pore size of the proteinosome by the length of the BS(PEG) $n$   
346 crosslinker. This provides a handle to tune the activity of the proteinosome by changing  
347 the one chemical in the methodology and without additional methodological steps.

348 The incorporation of cell free transcription and translation into proteinosomes  
349 provides an important tool for establishing synthetic cells with different architectural  
350 features. The porous membrane of the proteinosome and its ability to support  
351 transcription and translation could provide a minimal chemical model for isolating  
352 mRNA and DNA whilst allowing the diffusion of protein out of the proteinosomes and  
353 allowing the diffusion of resources into the proteinosome. The open nature of the  
354 proteinosome provides unique properties, *i.e.* resources can be continually supplied  
355 to the reaction to lengthen the time of the reaction. This is important for minimal  
356 systems which do not have the chemical complexity to autonomously produce energy  
357 from external resources that are required for the long-term sustenance of living  
358 systems.

359 Towards the goal of establishing synthetic cells from scratch the generation of multi  
360 compartments with different physical features can provide a route to replicate  
361 biological cellular architecture and to realise differential regulation of biochemical  
362 reactions. To this end,

363 We show that the native proteinosomes can support higher order architectural  
364 structures with a “Russian doll” effect where we generate a 3-tiered system with a  
365 condensate encapsulated within a proteinosome (Figure S18) which is encapsulated  
366 within a liposome. from the inclusion of small compartments based on protein (**Figure**  
367 **S18**) (**Figure 4**, **Figure S19**). Additional design elements that include the transport of  
368 mRNA out of the proteinosome to separate transcription and translation could be an  
369 intriguing property to include into the proteinosome – that more closely resembles  
370 some of the features of the cell nucleus for example.

371      Integration of cell free transcription and translation in robust synthetic cellular  
372      chassis, as we have demonstrated, is critical not only in providing tangible systems to  
373      build synthetic cells but is a fundamental requirement to address a key challenge  
374      within synthetic cellular research. The challenge to extend synthetic cellular systems  
375      from basic research to applications in the real world. For this, facile and reproducible  
376      methods and the ability to control and tune enzymatic activities are a fundamental  
377      prerequisite.

378

### 379      **Acknowledgements**

380      T.Y.D.T. and M.G. acknowledge financial support from the MPG and MaxSynBio  
381      Consortium, jointly funded by the Federal Ministry of Education and Research  
382      (Germany) and the Max Planck Society and the MPI-CBG. We thank the Deutsche  
383      Forschungsgemeinschaft (DFG, German Research Foundation) under Germany's  
384      Excellence Strategy – EXC-2068 – 390729961 – Cluster of Excellence Physics of Life  
385      of TU Dresden and EXC-1056- Center for Advancing Electronics Dresden;  
386      Volkswagen Stiftung for generous funding. We acknowledge the Light Microscopy  
387      Facility, the Electron Microscopy facility and the Protein Expression and Purification  
388      (PEPC) at MPI-CBG for assistance. We also acknowledge Delong instruments for the  
389      assistance of the TEM image acquisition. We thank David T. Gonzales for the help in  
390      preparing liposome. We also acknowledge Archishman Ghosh for the purified PRM5.  
391      We thank the Center for Macromolecular Structure Analysis in the Leibniz Institute of  
392      Polymer Research, Dresden for GPC analysis of the PNIPAAm chain.

393

394

### 395      **Author contributions**

396      M.G. and T.Y.D.T. conceived the research. M.G., D.W., M.W.-B., L.W. and J.S.  
397      contributed to the design of and the undertaking of the experiments. M.G., D.W., L.W.  
398      and J.S. analyzed the data. All authors contributed to the writing of the manuscript.

399 **Reference**

400 (1) Oberholzer, T.; Nierhaus, K. H.; Luisi, P. L. Protein Expression in Liposomes.  
401 Biochemical and Biophysical Research Communications 1999, 261 (2), 238–  
402 241. <https://doi.org/10.1006/bbrc.1999.0404>.

403 (2) Yu, W.; Sato, K.; Wakabayashi, M.; Nakaishi, T.; Ko-Mitamura, E. P.; Shima, Y.;  
404 Urabe, I.; Yomo, T. Synthesis of Functional Protein in Liposome. J Biosci  
405 Bioeng 2001, 92 (6), 590–593. <https://doi.org/10.1263/jbb.92.590>.

406 (3) Nishimura, K.; Tsuru, S.; Suzuki, H.; Yomo, T. Stochasticity in Gene Expression  
407 in a Cell-Sized Compartment. ACS Synth. Biol. 2015, 4 (5), 566–576.  
408 <https://doi.org/10.1021/sb500249g>.

409 (4) Chauhan, G.; Norred, S. E.; Dabbs, R. M.; Caveney, P. M.; George, J. K. V.;  
410 Collier, C. P.; Simpson, M. L.; Abel, S. M. Crowding-Induced Spatial  
411 Organization of Gene Expression in Cell-Sized Vesicles. ACS Synth. Biol. 2022.  
412 <https://doi.org/10.1021/acssynbio.2c00336>.

413 (5) Blanken, D.; Foschepoth, D.; Serrão, A. C.; Danelon, C. Genetically Controlled  
414 Membrane Synthesis in Liposomes. Nat Commun 2020, 11 (1), 4317.  
415 <https://doi.org/10.1038/s41467-020-17863-5>.

416 (6) Eto, S.; Matsumura, R.; Shimane, Y.; Fujimi, M.; Berhanu, S.; Kasama, T.;  
417 Kuruma, Y. Phospholipid Synthesis inside Phospholipid Membrane Vesicles.  
418 Commun Biol 2022, 5 (1), 1–11. <https://doi.org/10.1038/s42003-022-03999-1>.

419 (7) van Nies, P.; Westerlaken, I.; Blanken, D.; Salas, M.; Mencía, M.; Danelon, C.  
420 Self-Replication of DNA by Its Encoded Proteins in Liposome-Based Synthetic  
421 Cells. Nat Commun 2018, 9 (1), 1583. [https://doi.org/10.1038/s41467-018-03926-1](https://doi.org/10.1038/s41467-018-<br/>422 03926-1).

423 (8) Godino, E.; López, J. N.; Zarguit, I.; Doerr, A.; Jimenez, M.; Rivas, G.; Danelon,  
424 C. Cell-Free Biogenesis of Bacterial Division Proto-Rings That Can Constrict  
425 Liposomes. Commun Biol 2020, 3 (1), 1–11. [https://doi.org/10.1038/s42003-020-01258-9](https://doi.org/10.1038/s42003-<br/>426 020-01258-9).

427 (9) Noireaux, V.; Libchaber, A. A vesicle bioreactor as a step toward an artificial cell  
428 assembly. *Proc. Natl. Acad. Sci. USA* 2004, 101(51):17669-74.  
429 <https://doi.org/10.1073/pnas.0408236101>.

430 (10) Fragasso, A.; De Franceschi, N.; Stömmer, P.; van der Sluis, E. O.; Dietz, H.;  
431 Dekker, C. Reconstitution of Ultrawide DNA Origami Pores in Liposomes for  
432 Transmembrane Transport of Macromolecules. *ACS Nano* 2021, 15 (8), 12768–  
433 12779. <https://doi.org/10.1021/acsnano.1c01669>.

434 (11) Hindley, J. W.; Elani, Y.; McGilvery, C. M.; Ali, S.; Bevan, C. L.; Law, R. V.; Ces,  
435 O. Light-Triggered Enzymatic Reactions in Nested Vesicle Reactors. *Nat*  
436 *Commun* 2018, 9 (1), 1093. <https://doi.org/10.1038/s41467-018-03491-7>.

437 (12) Vogele, K.; Frank, T.; Gasser, L.; Goetzfried, M. A.; Hackl, M. W.; Sieber, S. A.;  
438 Simmel, F. C.; Pirzer, T. Towards Synthetic Cells Using Peptide-Based  
439 Reaction Compartments. *Nat Commun* 2018, 9 (1), 3862.  
440 <https://doi.org/10.1038/s41467-018-06379-8>.

441 (13) Nallani, M.; Andreasson-Ochsner, M.; Tan, C.-W. D.; Sinner, E.-K.; Wisantoso,  
442 Y.; Geifman-Shochat, S.; Hunziker, W. Proteopolymersomes: In Vitro  
443 Production of a Membrane Protein in Polymersome Membranes. *Biointerphases*  
444 2011, 6 (4), 153–157. <https://doi.org/10.1116/1.3644384>.

445 (14) Syeda, R.; Holden, M.A.; Hwang, W.L.; Bayley, H. Screening Blockers Against  
446 a Potassium Channel with a Droplet Interface Bilayer Array. *J. Am. Chem. Soc.*  
447 2008; 130(46): 15543-15548.

448 (15) Li, M.; Green, D. C.; Anderson, J. L. R.; Binks, B. P.; Mann, S. In Vitro Gene  
449 Expression and Enzyme Catalysis in Bio-Inorganic Protocells. *Chem. Sci.* 2011,  
450 2 (9), 1739–1745. <https://doi.org/10.1039/C1SC00183C>.

451 (16) Sokolova, E.; Spruijt, E.; Hansen, M. M. K.; Dubuc, E.; Groen, J.;  
452 Chokkalingam, V.; Piruska, A.; Heus, H. A.; Huck, W. T. S. Enhanced  
453 Transcription Rates in Membrane-Free Protocells Formed by Coacervation of  
454 Cell Lysate. *Proc. Natl. Acad. Sci. U.S.A.* 2013, 110 (29), 11692–11697.  
455 <https://doi.org/10.1073/pnas.1222321110>.

456 (17) Weiss, M.; Frohnmayer, J. P.; Benk, L. T.; Haller, B.; Janiesch, J.-W.; Heitkamp,  
457 T.; Börsch, M.; Lira, R. B.; Dimova, R.; Lipowsky, R.; Bodenschatz, E.; Baret, J.-  
458 C.; Vidakovic-Koch, T.; Sundmacher, K.; Platzman, I.; Spatz, J. P. Sequential  
459 Bottom-up Assembly of Mechanically Stabilized Synthetic Cells by Microfluidics.  
460 *Nature Mater* 2018, 17 (1), 89–96. <https://doi.org/10.1038/nmat5005>.

461 (18) Niederholtmeyer, H.; Chaggan, C.; Devaraj, N. K. Communication and Quorum  
462 Sensing in Non-Living Mimics of Eukaryotic Cells. *Nat Commun* 2018, 9 (1),  
463 5027. <https://doi.org/10.1038/s41467-018-07473-7>.

464 (19) J. Whitfield, C.; M. Banks, A.; Dura, G.; Love, J.; E. Fieldsend, J.; A. Goodchild,  
465 S.; A. Fulton, D.; P. Howard, T. Cell-Free Protein Synthesis in Hydrogel  
466 Materials. *Chemical Communications* 2020, 56 (52), 7108–7111.  
467 <https://doi.org/10.1039/D0CC02582H>.

468 (20) Ouyang, X.; Zhou, X.; Lai, S. N.; Liu, Q.; Zheng, B. Immobilization of Proteins of  
469 Cell Extract to Hydrogel Networks Enhances the Longevity of Cell-Free Protein  
470 Synthesis and Supports Gene Networks. *ACS Synthetic Biology* 7.

471 (21) Zambrano, A.; Fracasso, G.; Gao, M.; Ugrinic, M.; Wang, D.; Appelhans, D.;  
472 deMello, A.; Tang, T.-Y. D. Programmable Synthetic Cell Networks Regulated  
473 by Tuneable Reaction Rates. *Nat Commun* 2022, 13 (1), 3885.  
474 <https://doi.org/10.1038/s41467-022-31471-5>.

475 (22) Yang, S.; Joesaar, A.; Bögels, B. W. A.; Mann, S.; de Greef, T. F. A.  
476 Protocellular CRISPR/Cas-Based Diffusive Communication Using  
477 Transcriptional RNA Signaling. *Angew Chem Int Ed* 2022, 61 (26).  
478 <https://doi.org/10.1002/anie.202202436>.

479 (23) Joesaar, A.; Yang, S.; Bögels, B.; van der Linden, A.; Pieters, P.; Kumar, B.P.;  
480 Dalchau, N.; Phillips, A.; Mann, S.; de Greef, T.F. DNA-based communication in  
481 populations of synthetic protocells. *Nat. Nanotechnol.* 14, 369–378 (2019).  
482 <https://doi.org/10.1038/s41565-019-0399-9>

483 (24) Zhou, P.; Liu, X.; Wu, G.; Wen, P.; Wang, L.; Huang, Y.; Huang, X.  
484       Programmable Modulation of Membrane Permeability of Proteinosome upon  
485       Multiple Stimuli Responses. *ACS Macro Letters* 2016, 6.

486 (25) Huang, X.; Li, M.; Mann, S. Membrane-Mediated Cascade Reactions by  
487       Enzyme–Polymer Proteinosomes. *Chem. Commun.* 2014, 50 (47), 6278–6280.  
488       <https://doi.org/10.1039/C4CC02256D>.

489 (26) Gobbo, P.; Patil, A. J.; Li, M.; Harniman, R.; Briscoe, W. H.; Mann, S.  
490       Programmed Assembly of Synthetic Protocells into Thermoresponsive  
491       Prototissues. *Nature Mater* 2018, 17 (12), 1145–1153.  
492       <https://doi.org/10.1038/s41563-018-0183-5>.

493 (27) Wang, L.; Wen, P.; Liu, X.; Zhou, Y.; Li, M.; Huang, Y.; Geng, L.; Mann, S.;  
494       Huang, X. Single-Step Fabrication of Multi-Compartmentalized Biphasic  
495       Proteinosomes. *Chem. Commun.* 2017, 53 (61), 8537–8540.  
496       <https://doi.org/10.1039/C7CC04180B>.

497 (28) Liu, X.; Zhou, P.; Huang, Y.; Li, M.; Huang, X.; Mann, S. Hierarchical  
498       Proteinosomes for Programmed Release of Multiple Components. *Angewandte  
499       Chemie* 2016, 128 (25), 7211–7216. <https://doi.org/10.1002/ange.201601427>.

500 (29) Jiang, Y.; Zhang, X.; Yuan, H.; Huang, D.; Wang, R.; Liu, H.; Wang, T.  
501       Research Progress and the Biotechnological Applications of Multienzyme  
502       Complex. *Appl Microbiol Biotechnol* 2021, 105 (5), 1759–1777.  
503       <https://doi.org/10.1007/s00253-021-11121-4>.

504 (30) Wang, P.; Moreno, S.; Janke, A.; Boye, S.; Wang, D.; Schwarz, S.; Voit, B.;  
505       Appelhans, D. Probing Crowdedness of Artificial Organelles by Clustering  
506       Polymersomes for Spatially Controlled and PH-Triggered Enzymatic Reactions.  
507       *Biomacromolecules* 2022. <https://doi.org/10.1021/acs.biomac.2c00546>.

508 (31) Heidari, A.; Sentürk, O. I.; Yang, S.; Joesaar, A.; Gobbo, P.; Mann, S.; de Greef,  
509       T. F. A.; Wegner, S. V. Orthogonal Light-Dependent Membrane Adhesion  
510       Induces Social Self-Sorting and Member-Specific DNA Communication in

511        Synthetic Cell Communities. *Small* n/a (n/a), 2206474.  
512        <https://doi.org/10.1002/smll.202206474>.

513        (32) Ugrinic, M.; Zambrano, A.; Berger, S.; Mann, S.; Tang, T.-Y. D.; deMello, A.  
514        Microfluidic Formation of Proteinosomes. *Chem. Commun.* 2018, 54 (3), 287–  
515        290. <https://doi.org/10.1039/C7CC08466H>.

516        (33) Huang, X.; Li, M.; Green, D. C.; Williams, D. S.; Patil, A. J.; Mann, S. Interfacial  
517        Assembly of Protein–Polymer Nano-Conjugates into Stimulus-Responsive  
518        Biomimetic Protocells. *Nat Commun* 2013, 4 (1), 2239.  
519        <https://doi.org/10.1038/ncomms3239>.

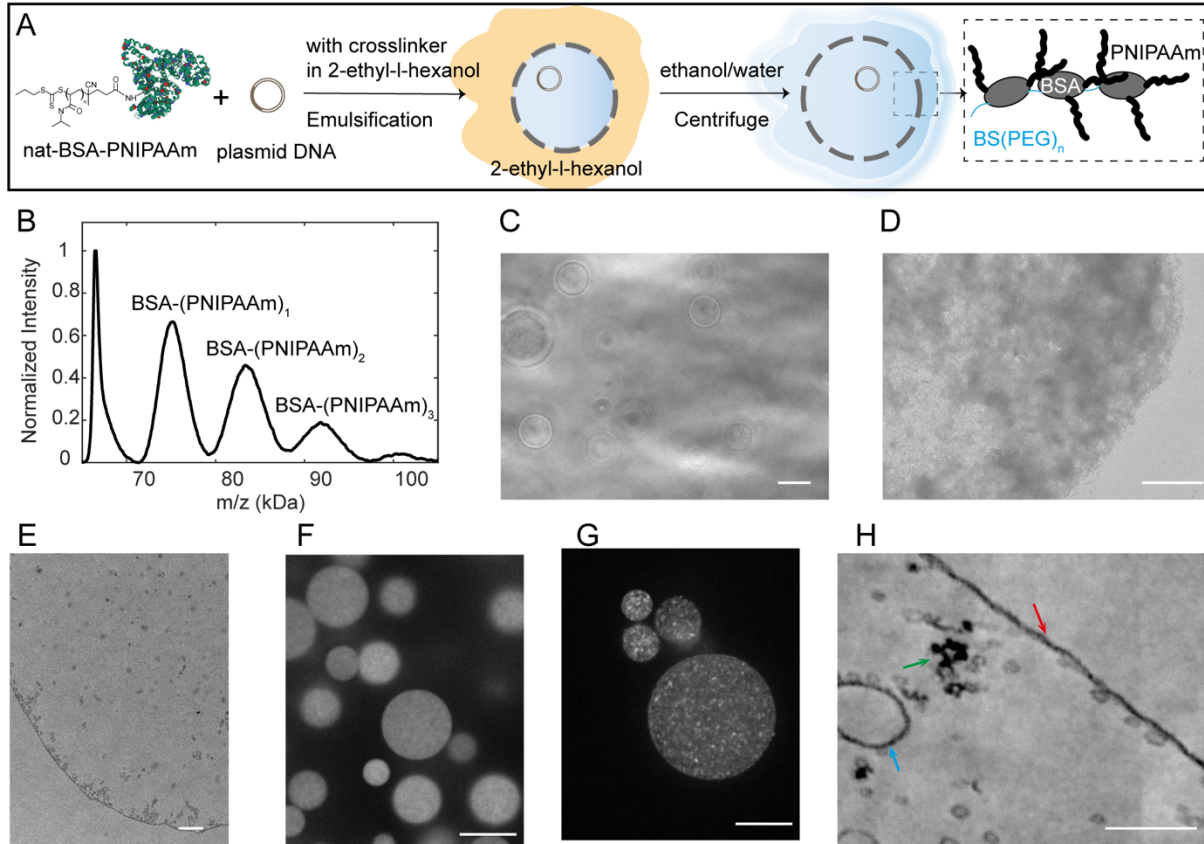
520        (34) O. Peetz, N. Hellwig, E. Henrich, J. Mezhyrova, V. Dötsch, F. Bernhard, N.  
521        Morgner, *J. Am. Soc. Mass Spectrom.* 2019, 30, 181.

522        (35) Gonzales, D. T.; Yandrapalli, N.; Robinson, T.; Zechner, C.; Tang, T.-Y. D. Cell-  
523        Free Gene Expression Dynamics in Synthetic Cell Populations. *ACS Synth.*  
524        *Biol.* 2022, 11 (1), 205–215. <https://doi.org/10.1021/acssynbio.1c00376>.

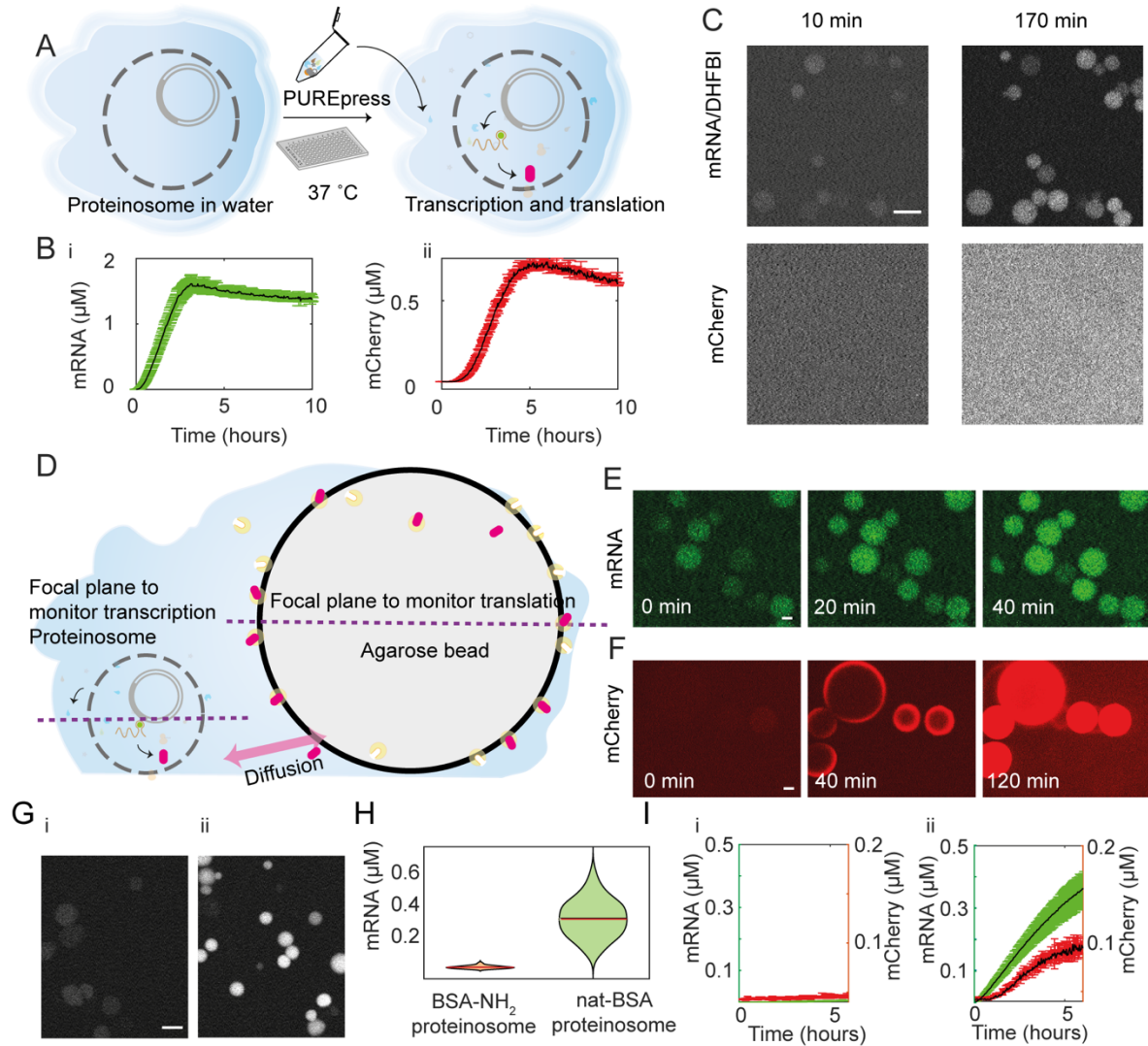
525        (36) J. Schindelin, I. Arganda-Carreras, E. Frise, V. Kaynig, M. Longair, T. Pietzsch,  
526        S. Preibisch, C. Rueden, S. Saalfeld, B. Schmid, J.-Y. Tinevez, D. J. White, V.  
527        Hartenstein, K. Eliceiri, P. Tomancak, A. Cardona, *Nat. Methods* 2012, 9, 676.

528        (37) N. Kempf, C. Remes, R. Ledesch, T. Züchner, H. Höfig, I. Ritter, A. Katranidis,  
529        J. Fitter, *Sci. Rep.* 2017, 7, 46753.

530 **Figures**



531  
532 **Figure 1:** Preparation and characterization of native BSA proteinosomes. A)  
533 Schematic describing the preparation of the native proteinosomes. Nat-BSA-  
534 PNIPAAm and plasmid DNA are mixed in 0.1 M sodium bicarbonate (NaHCO<sub>3</sub>, pH 8.4)  
535 aqueous phase and mixed with 2-ethyl-1-hexanol containing BS(PEG)<sub>n</sub> generating  
536 emulsions. After crosslinking, step-wisely purified from oil to water. B) Laser induced  
537 liquid beam ion desorption (LILBID) mass-spectra of nat-BSA-PNIPAAm. The average  
538 distance between multiple BSA-(PNIPAAm)<sub>n</sub> peaks was calculated to be 8.4 kDa. C)  
539 Phase-contrast microscopy image of empty nat-BSA proteinosomes. Scale bar: 20  $\mu$ m.  
540 D) Transmission electron microscope (TEM) image of a part of an empty nat-BSA  
541 proteinosome negatively stained with 1% uranyl acetate. Scale bar: 1  $\mu$ m. E) TEM  
542 image of part of an empty nat-BSA proteinosome embedded in resin and cross-  
543 sectioned to a thickness of 70  $\mu$ m. Scale bar: 1  $\mu$ m. TEM images were obtained on a  
544 Tecnai 12 TEM. F) Fluorescence microscopy images showing plasmid DNA  
545 encapsulated within nat-BSA proteinosomes. G) Fluorescence microscopy images  
546 showing plasmid DNA encapsulated within BSA-NH<sub>2</sub> proteinosome. Proteinosomes in  
547 F and G were stained with DNA dye EvaGreen and the images were obtained using a  
548 spinning disk microscope with a 60x/1.3 NA UPLSAPO objective. Scale bars in E and  
549 F: 10  $\mu$ m. H) TEM image of a plasmid DNA contained nat-BSA proteinosome  
550 incubated with diluted PURExpress. The proteinosome sample was embedded in resin,  
551 cross-sectioned to a thickness of 70  $\mu$ m and imaged on a Delong TEM at 25 kV. Red  
552 arrows refer to the proteinosome membrane, green arrow points to plasmid DNA,  
553 blue arrow points to small compartments. Scale bar: 100 nm. The images shown are  
554 representations of at least three experimental replicates. The replicates can be found  
555 in the data archive.

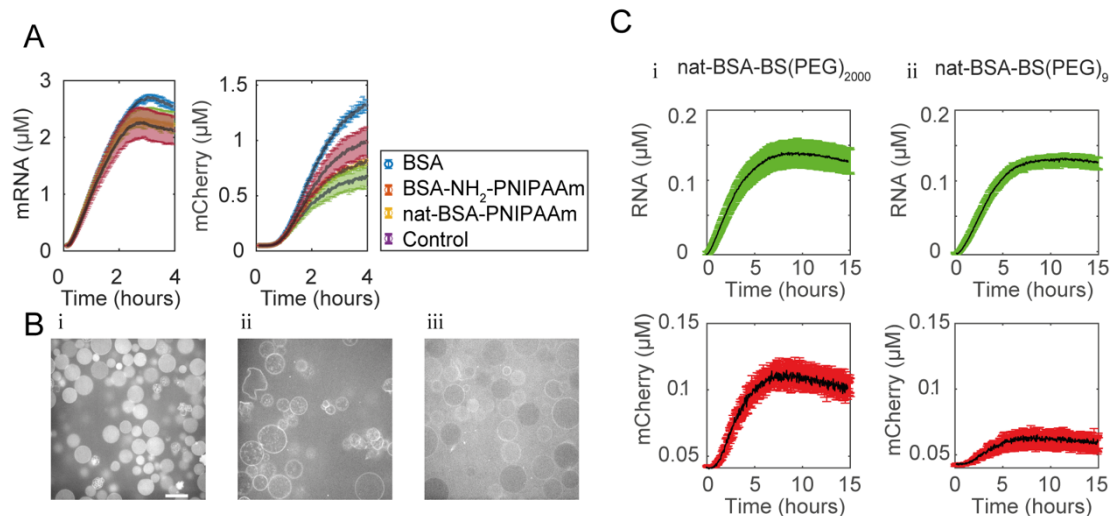


556  
557

558 **Figure 2:** Cell free expression within BSA proteinosomes A) Schematic of  
559 experimental work flow for cell free expression within proteinosomes. Proteinosome in  
560 aqueous phase were mixed with PUREExpress and imaged on a microplate reader. B)  
561 The kinetics of transcription of mRNA (i) and translation of mCherry (ii) were measured.  
562 C) Confocal microscopy images of nat-BSA proteinosomes containing plasmid DNA  
563 incubated with PUREExpress after 10 mins and 170 mins. Scale bar: 10  $\mu\text{m}$ . D)  
564 Schematic showing the incorporation of RFP trap with proteinosomes to confirm  
565 protein expression. Proteinosomes and the agarose beads-based RFP trap were  
566 imaged with confocal microscopy at different focal planes. E) Confocal microscopy  
567 images of DNA transcription in a dispersion of proteinosomes. F) The corresponding  
568 mCherry signals from the agarose beads in the same field of view but at different focal  
569 plane. G) Confocal microscopy images showing mRNA production in BSA-NH<sub>2</sub>  
570 proteinosome (i) and nat-BSA proteinosome (ii) with PUREExpress (0.33x) after 3 hours.

571 H) The DHFBI/mRNA signal distribution extracted from G. Red line represents the  
572 mean value. I) Cell free expression in BSA-NH<sub>2</sub> proteinosome (i) or nat-BSA  
573 proteinosome with PURExpress (0.33x) (ii), where transcription (green) and  
574 translation (red) were monitored with a Tecan Spark 20M microplate reader. Scale bar:  
575 10  $\mu$ m. All experiments were undertaken at 37 °C. 3 repeats were performed and the  
576 shade were plotted as mean (black line)  $\pm$ standard deviation. All microscopy images  
577 are representations of the results obtained from replicate experiments.

578



579  
580 **Figure 3:** A) Cell free transcription (i) and translation (ii) in the presence of 1 mg.mL<sup>-1</sup>  
581 of BSA (blue), BSA-NH<sub>2</sub>-PNIPAAm (orange) or nat-BSA-PNIPAAm (yellow) and a  
582 buffer control (purple) with PURExpress containing plasmid DNA (2.7 nM).  
583 Transcription (i) and translation (ii) were monitored via mRNA/DHFBI and mCherry  
584 respectively on a microplate reader. B) Permeability of labeled ribosomes into  
585 proteinosomes with DNA plasmid. Ribosomes were prepared in ribosome  
586 resuspension buffer and incubated with nat-BSA proteinosome crosslinked with  
587 BS(PEG)<sub>2000</sub> (i); BSA-NH<sub>2</sub> proteinosome crosslinked with BS(PEG)<sub>2000</sub> (ii), and BSA-  
588 NH<sub>2</sub> proteinosome crosslinked with BS(PEG)<sub>9</sub> (iii). Cy5 labeled ribosome was imaged  
589 on a laser scanning confocal microscope with a 63x/1.3 NA Plan-Apochromat  
590 objective. C) Kinetics of transcription (green) and translation (red) in nat-BSA  
591 proteinosome crosslinked with BS(PEG)<sub>2000</sub> (i) and BS(PEG)<sub>9</sub> (ii) incubated with  
592 PURExpress (0.5x) monitored on a microplate reader at 37°C. 3 repeats were  
593 performed and the shade were plotted as mean (black line)  $\pm$ standard deviation. All  
594 microscopy images are representations of the results obtained from replicate  
595 experiments.